Stronger speed limit for observables: Tighter bound for the capacity of entanglement, the modular Hamiltonian, and the charging of a quantum battery

Divyansh Shrimali [1,*] Biswaranjan Panda,[2,3,†] and Arun Kumar Pati[3,‡]

[1]*Harish Chandra Research Institute, A CI of Homi Bhabha National Institute, Chhatnag Road, Jhunsi, Prayagraj 211019, India*

[2]*Indian Institute of Science Education and Research (IISER), Berhampur, Odisha 760010, India*

[3]*Center for Quantum Engineering, Research and Education (CQuERE), TCG CREST, Kolkata 700091, India*

(Received 6 April 2024; accepted 1 August 2024; published 15 August 2024)

How fast an observable can evolve in time is answered by so-called observable speed limit. Here, we prove a stronger version of the observable speed limit and show that the previously obtained bound is a special case of the new bound. The stronger quantum speed limit for the state also follows from the stronger quantum speed limit for observables (SQSLO). We apply this to prove a stronger bound for the entanglement rate using the notion of capacity of entanglement (the quantum information theoretic counterpart of the heat capacity) and show that it outperforms previous bounds. Furthermore, we apply the SQSLO for the rate of modular Hamiltonian and in the context of interacting qubits in a quantum battery. These illustrative examples reveal that the speed limit for the modular energy and the time required to charge the battery can be exactly predicted using the new bound. This shows that for estimating the charging time of quantum battery SQSLO is actually tight, i.e., it saturates. Our findings can have important applications in quantum thermodynamics, the complexity of operator growth, predicting the time rate of quantum correlation growth, and quantum technology, in general.

DOI: 10.1103/PhysRevA.110.022425

I. INTRODUCTION

Since the inception of scientific explorations, time has remained a paramount and fundamental notion in the study of physical systems. However, understanding time presents a considerable challenge, as it is not an operator but rather a parameter. New insights on the nature of time emerged after the formulation of the geometric uncertainty relation between energy fluctuation and time, imposing limitations on the rate at which a quantum system evolves. This concept was later formalized as the quantum speed limit (QSL), which delineates the minimal time required for the evolution of a quantum system. The Mandelstam and Tamm derived a time-energy uncertainty relation that bounds the speed of evolution in terms of the energy dispersion [1]. And some years later, another speed limit was identified for quantum state evolution, which incorporates the average energy in the ground state of the Hamiltonian [2,3]. There exist few protocols involving quantum controls also that have been utilized to provide optimal value and controls to reach the target state within minimum time for entanglement production [4] and charging of quantum batteries [5–7]. Our work in this paper though strictly relates with QSL, which depends on the shortest path connecting the initial and final states of a given quantum system, which depends on the fluctuation in the Hamiltonian and thus provides crucial insights into the dynamics of quantum processes.

During the nascent stages of research, the bounds of the QSL were primarily established for the unitary dynamics of pure states for quantum systems [1–3,8–28]. Subsequently, researchers delved into investigating QSL within the framework of unitary dynamics for mixed states [29–38]. The significance of QSL extends beyond theoretical explorations as it plays a pivotal role in the advancement of quantum technologies and devices, among other applications. Indeed, QSL finds diverse applications, including but not limited to, quantum computing [39], quantum thermodynamics [40,41], quantum control theory [42,43], quantum metrology [44], and beyond.

Later, following the discovery of the stronger uncertainty relation Ref. [45], a more robust QSL was unveiled [46], which presented a tighter bound than the previously established Mandelstam and Tamm (MT) and Margolus-Levitin (ML) bounds. These advancements were made within the Schrödinger picture, where the state vector evolves over time. Subsequently, the exploration of QSL within the Heisenberg picture where observables evolve in time rather than the state, gathered interest.

Henceforth, leveraging the Robertson-Schrödinger uncertainty for observables utilizing Mandelstam and Tamm (MT) bound, a novel QSL bound was established, which is termed as the quantum speed limit for observables (QSLO) [47]. This development prompted a natural inquiry: could we derive another bound using the stronger uncertainty relation? This question arises because the SQSL is already tighter than the MT bound, and while the QSLO is approximately equally as tight as the MT bound, there remains a need for a tighter

*Contact author: divyanshshrimali@hri.res.in

†Contact author: biswaranjanpanda2002@gmail.com

‡Contact author: arun.pati@tcgcrest.org

bound for observables in the Heisenberg picture. Indeed, not only have we derived this new stronger bound, but have shown that it gives a significant improvement over QSLO while examining few prominent examples provided in this paper.

Entanglement is considered a very useful resource in information-processing tasks. Hence over the years, how to create and quantify entanglement has been a subject of major exploration [48,49]. The creation of quantum entanglement between two particles depends upon the choice of the initial state and suitable nonlocal interaction between them, but the designing of suitable interacting Hamiltonian is not always easy, which renders the production of entanglement a nontrivial task. Thus, for a given nonlocal Hamiltonian, what can be the best way to utilize this Hamiltonian to create entanglement? One way to answer this query is by making use of the capacity of entanglement that was originally proposed to characterize topologically ordered states in the context of Kitaev model [50]. For a given pure bipartite entangled state ρ_{AB}, the capacity of entanglement is defined as the second cumulant of the entanglement spectrum, i.e., associated with the reduced density matrix, with $\{\lambda_i\}'$s, the eigenvalues of the reduced density matrix of any one of the subsystem, the capacity of entanglement C_{E} is defined as the second cumulant of this entanglement spectrum, i.e; $C_{\mathrm{E}} = \sum_i \lambda_i \log_2^2 \lambda_i - S_{\mathrm{EE}}^2$, where $S_{\mathrm{EE}} = -\sum_i \lambda_i \log_2 \lambda_i$ is the well-known entanglement entropy. C_{E} is similar in form to the heat capacity of thermal systems and can be thought of as the variance of the distribution of $-\log_2 \lambda_i$ with probability λ_i and hence contains information about the width of the eigenvalue distribution of reduced density matrix. It was shown in Ref. [51] that the quantum speed limit for creating the entanglement depends inversely on the fluctuation in the nonlocal Hamiltonian as well as on the average of the square root of the capacity of entanglement. It was, thus, inferred that the more the capacity of entanglement, the shorter the time duration system may take to produce the desired amount of entanglement.

Our first illustration involves readdressing the entanglement rate, which was bounded by fluctuation in the nonlocal Hamiltonian and the capacity of entanglement as defined in Ref. [50]. It is to be seen whether we can achieve a tighter bound for entanglement generation or degradation with the stronger uncertainty relation. If so, what can be the physical implication for the new expression, and under what choice of parameters we can achieve a tighter bound for a greater duration? Furthermore, a similar object was studied under the Heisenberg picture and the subsequent bound was interpreted in the form of the generation of modular energy, defined in the present context as a mean of composite modular Hamiltonian. Needless to say, the notion of capacity of entanglement has applications in diverse areas of physics ranging from condensed matter systems [52] to conformal field theories [50,53], and alike.

For the final example case, we analyze the ergotropy and bound on the charging process of quantum batteries. The various traditional batteries we make use of such as lithium-ion, alkaline, and lead-acid batteries operate based on electrochemical reactions involving the movement of electrons between two electrodes through electrolytes. The performance of these batteries depends on factors such as electrolyte composition, electrode materials, and overall design. The quantum batteries (QBs) represent a new frontier, grounded in quantum mechanical principles such as tunneling effects, entanglement, qubit-based technologies, and more [54]. Theoretical models propose that these batteries can leverage quantum superposition and entanglement to store and recover energy, offering enhanced efficiency compared to conventional batteries [55–60]. However, despite their potential advantages, QBs are still in the early stages of development due to technological limitations. Numerous challenges, including issues related to stability, scalability, and practical implementation, need to be addressed for their widespread usage [61,62].

The QB model comprises two essential components: a battery charger and a battery holder. However, energy loss is also accounted for in the subsequent stages, achievable by isolating the quantum system from the environment, treated as a dissipationless subsystem. The effective coupling of the battery holder with the battery charger is crucial for energy acquisition. The focus of recent theoretical research has been on exploring basic bipartite state models and other related models in the realm of quantum batteries [63–81]. Theoretical evidence already supports the notion that in a collective charging scheme, QBs can demonstrate accelerated charging leveraging quantum correlations [55,56,82]. Presently, diverse models of QBs have been proposed, including quantum cavities, spin chains, the Sachdev-Ye-Kitaev model and quantum oscillators [61,68,83–93]. However, experimental investigations are limited, with fewer models explored, such as the cavity-assisted charging of an organic quantum battery [94]. In this paper, we take the example of entanglement-based QBs under different charging regimes. It is examined whether stronger quantum speed limit for observables (SQSLO) gives any significant improvement over existing QSLO [47,95] for charging time.

This paper is organized as follows. In Sec. II, we discuss all the basic concepts utilized in this paper. Subsequently, in Sec. III, we derive the SQSLO bound by employing a stronger uncertainty relation and compare it with other previously established bounds. In the next Sec. IV, we have given the SQSL for states and demonstrated a better bound for entanglement generation with capacity of entanglement. Following this, in Sec. V, we present two applications of the QSLO bound for the modular energy and charging time of the quantum battery. Finally, in Sec. VI, we conclude our paper.

II. DEFINITIONS AND RELATIONS

Stronger uncertainty relation. Unlike classical systems, where all observables can be measured with arbitrary accuracy, the same is not true for quantum systems. For a given quantum state there are restrictions on the results of the measurements of noncommuting observables. The uncertainty relation captures such a restriction for two incompatible observables.

The Heisenberg-Robertson uncertainty relation provides a lower bound by merely yielding the product of two variances of observables based on their commutator. This proves that it is impossible to prepare a quantum state for which variances of two noncommuting observables can be arbitrarily reduced simultaneously. In contrast, a stronger uncertainty relation offers a more comprehensive approach by

considering the sum of variances. This approach ensures that the lower bound remains nontrivial, especially when dealing with two observables that are incompatible within the state of the system. Thus, it provides a more nuanced understanding of uncertainty, particularly in cases where traditional relations fall short. However, we will not be using the sum form of the stronger uncertainty relation. One of the stronger uncertainty relations in the product form as given in Ref. [45] has the form

$$\Delta A\Delta B \geqslant \pm\frac{i}{2}\frac{\langle[A,B]\rangle}{\left(1-\frac{1}{2}\left|\langle\Psi^{\perp}|\frac{A}{\Delta A}\mp i\frac{B}{\Delta B}|\Psi\rangle\right|^2\right)}, \tag{1}$$

where A and B are two incompatible observables with $\Delta A = \sqrt{\langle A^2\rangle - \langle A\rangle^2}$, $\Delta B = \sqrt{\langle B^2\rangle - \langle B\rangle^2}$, and the averages are defined in the state $|\Psi\rangle$ for the given quantum system. This Eq. (1) can be reduced to the Heisenberg-Robertson uncertainty relation when it minimizes the lower bound over $|\Psi^{\perp}\rangle$ and becomes an equality when it maximizes it. The above relation is stronger than the standard Heisenberg-Robertson uncertainty relation. We will be using this to prove our stronger quantum speed limit for observables.

Capacity of entanglement. Let us consider a composite system AB with pure state $|\Psi\rangle_{AB}$. The amount of entanglement between subsystems A and B can be quantified via the entanglement entropy, which is defined as the von Neumann entropy of the reduced density operator $\rho_A = \sum_n \lambda_n |\psi_n\rangle_A \langle\psi_n|$ (or ρ_B), i.e.,

$$S_{\rm EE} = S(\rho_A) = -\operatorname{tr}(\rho_A \log_2 \rho_A) = -\sum_n \lambda_n \log_2 \lambda_n, \tag{2}$$

which is invariant under local unitary transformations on ρ_A. The von Neumann entropy vanishes when density operator ρ_A is a pure state. For a completely mixed density operator, the von Neumann entropy attains its maximum value of $\log_2 \mathrm{d_A}$, where $\mathrm{d_A} = \dim(\mathcal{H}_A)$.

For any density operator ρ_A associated with quantum system A, we can define a formal Hamiltonian K_A, called the modular Hamiltonian, with respect to which the density operator ρ_A is a Gibbs-like state (with $\beta = 1$)

$$\rho_A = \frac{e^{-K_A}}{Z},$$

where $Z = \operatorname{tr}(e^{-K_A})$. Note that any density matrix can be written in this form for some choice of Hermitian operator K_A. With slight adjustments in the above equation, the modular Hamiltonian K_A can be written as $K_A = -\log_2 \rho_A$. In this case, the entanglement entropy of the system is equivalent to the thermodynamic entropy of a system described by Hamiltonian K_A (with $\beta = 1$). Writing in terms of modular Hamiltonian $K_A = -\log_2 \rho_A$, the entanglement entropy becomes the expectation value of the modular Hamiltonian

$$S_{\rm EE} = -\operatorname{tr}(\rho_A \log_2 \rho_A) = \operatorname{tr}(\rho_A K_A) = \langle K_A\rangle. \tag{3}$$

The capacity of entanglement is another information-theoretic quantity that has gained some interest in recent time [96]. It is defined as the variance of the modular Hamiltonian K_A [50] in the state $|\Psi\rangle_{AB}$ and can be expressed as

$$\begin{aligned} C_{\rm E}(\rho_A) &= \langle\Psi|\,(K_A\otimes\mathcal{I}_B)^2\,|\Psi\rangle - \langle\Psi|\,(K_A\otimes\mathcal{I}_B)\,|\Psi\rangle^2 \\ &= \operatorname{tr}[\rho_A(-\log_2\rho_A)^2] - [\operatorname{tr}(-\rho_A\log_2\rho_A)]^2 \\ &= \operatorname{tr}\left[\rho_A K_A^2\right] - [\operatorname{tr}(\rho_A K_A)]^2 \\ &= \langle K_A^2\rangle - \langle K_A\rangle^2 = \Delta K_A^2. \end{aligned} \tag{4, 5}$$

The capacity of entanglement has also been defined in terms of variance of the relative surprisal between two density matrices $V(\rho||\sigma)$:

$$V(\rho||\sigma) = \operatorname{tr}(\rho[\log_2(\rho) - \log_2(\sigma)]^2) - D(\rho||\sigma)^2. \tag{6}$$

Here, if one of the density matrices becomes maximally mixed (i.e., either ρ or σ becomes $\mathcal{I}/d$), then the variance of the relative surprisal becomes the capacity of entanglement. For further details and properties of capacity of entanglement, readers are advised to go through Ref. [97].

Extractable work from quantum batteries. Let the quantum system representing the battery be of dimension d with the corresponding Hilbert space $\mathcal{H}$. We further pick a standard basis for describing the system Hamiltonian

$$H = \sum_{j=1}^{d} h_j |j\rangle\langle j| \quad \text{with} \quad h_{j+1} > h_j, \tag{7}$$

where the assumption is that the energy levels are nondegenerate.

To extract the energy from the battery, the time-dependent fields that are used can be described as $V(t) = V^{\dagger}(t)$ where such fields are switched on for time interval $0 \geqslant t \geqslant \tau$. The initial state of the battery is described by a density matrix ρ, which is evolved from the Liouville equation

$$\frac{d}{dt}\rho(t) = -i[H + V(t), \rho(t)], \quad \rho(0) = \rho. \tag{8}$$

The work extraction by this procedure is then

$$W = \operatorname{tr}(\rho H) - \operatorname{tr}[\rho(\tau)H], \tag{9}$$

where time-evolved state is given as $\rho(\tau) = U(\tau)\,\rho\,U^{\dagger}(\tau)$.

Further, through a proper choice of V, any unitary U can be obtained for $U(\tau)$. Therefore the maximal amount of extractable work, called ergotropy, can be defined as

$$W_{\max} := \operatorname{tr}(\rho H) - \min \operatorname{tr}(U\rho U^{\dagger}H), \tag{10}$$

where the minimum is taken over all unitary transformations of $\mathcal{H}$.

III. STRONGER QSL FOR OBSERVABLES (SQSLO)

Derivation of stronger quantum speed limit for observables

Let us consider a quantum system with a state vector $|\Psi\rangle \in \mathcal{H}^N$. In the Heisenberg picture, we can imagine that the operators representing the observables evolve in time, while the vectors in the Hilbert space (quantum states) remain independent of time. This is opposite to the Schrödinger picture, where the observables are independent of time and the states evolve in time. In the Heisenberg picture, each self-adjoint operator evolves in time according to the operator-valued differential equation.

As we are dealing with the Heisenberg picture, the observable $O(t)$ undergoes a unitary evolution as given by the

Heisenberg equation of motion

$$i\hbar\frac{dO(t)}{dt} = [O(t), H], \tag{11}$$

where H is the Hamiltonian operator of the system, and where $[O, H]$ is the commutator. If $O(t)$ commutes with the Hamiltonian, then it remains constant in time. In this section, we aim to derive a more stringent QSL bound for observables, surpassing the previously obtained limit. This bound stems from the stronger uncertainty relation, applicable to any two incompatible observables $A(t)$ and $B(t)$ in the Heisenberg picture. This is given by

$$\Delta A(t)\ \Delta B(t)\ [1 - R(t)] \geqslant \pm\frac{i}{2}\langle\Psi|[A(t), B(t)]|\Psi\rangle, \tag{12}$$

where

$$R(t) = \frac{1}{2}\left|\langle\Psi^{\perp}|\frac{A(t)}{\Delta A(t)} \mp i\frac{B(t)}{\Delta B(t)}|\Psi\rangle\right|^2, \tag{13}$$

$\Delta A(t) = \sqrt{\langle A(t)^2\rangle - \langle A(t)\rangle^2}$, $\Delta B(t) = \sqrt{\langle B(t)^2\rangle - \langle B(t)\rangle^2}$, $|\Psi\rangle$ is the state of the system in which averages are calculated and $|\Psi^{\perp}\rangle$ is the orthogonal state to $|\Psi\rangle$. We will prove that the bound obtained from the above equation is tighter than the existing bound T_{QSLO}, which was derived by using Robertson uncertainty relation.

Now, consider the desired observable, denoted as $A = O(t)$, and an another operator, $B = H$. Using the stronger uncertainty relation, we can obtain

$$\Delta O(t)\ \Delta H\ (1 - R(t)) \geqslant \frac{\hbar}{2}\left|\frac{d\langle O(t)\rangle}{dt}\right|. \tag{14}$$

From the above expression, we obtain the stronger quantum speed limit for observable (SQSLO) as given by

$$T \geqslant T^{O}_{\mathrm{SQSL}} = \frac{\hbar}{2\Delta H}\int_0^T \frac{|d\langle O(t)\rangle|}{\Delta O(t)\ \eta(t)}, \tag{15}$$

where $\eta(t) = (1 - R(t))$, $\Delta O(t) = \sqrt{\langle O(t)^2\rangle - \langle O(t)\rangle^2}$ and $\Delta H = \sqrt{\langle H^2\rangle - \langle H\rangle^2}$. Here, the time T denotes the time we consider for the evolution of quantum system. This SQSLO can be written as

$$T^{O}_{\mathrm{SQSL}} = \frac{\hbar}{2\Delta H}\frac{|\langle O(T)\rangle - \langle O(0)\rangle|}{\langle\langle\Delta O(t)\ \eta(t)\rangle\rangle_T}, \tag{16}$$

where $\langle\langle\Delta O(t)\ \eta(t)\rangle\rangle_T = \frac{1}{T}\int_0^T \Delta O(T)\ \eta(t)dt$, is the time average of the quantity $\Delta O(t)\ \eta(t)$ [98].

Alternatively, through Eq. (14), we can rewrite SQSLO as

$$T \geqslant T^{O}_{\mathrm{SQSL}} = \frac{\hbar\ \Lambda(T)}{2\Delta H}\int_0^T \frac{|d\langle O(t)\rangle|}{\Delta O(t)}, \tag{17}$$

where $\Lambda(T) = \frac{1}{1-\overline{R}(t)}$, with $\overline{R}(t) = \frac{1}{T}\int_0^T R(t)\ dt$.

Now, we can show that the previously derived bound of the QSLO [47] follows from the stronger QSLO. This will ensure that SQSLO is an improvement over QSLO. As evident from Eq. (15), an additional factor of $\eta(t) = 1 - R(t)$ is present in SQSLO, with $0 \leqslant R(t) \leqslant 1\ \forall\ t$, we have $\eta(t) \in [0, 1]$. This results in the final expression

$$T \geqslant \frac{\hbar}{2\Delta H}\int_0^T \frac{|d\langle O(t)\rangle|}{\Delta O(t)\eta(t)} \geqslant \frac{\hbar}{2\Delta H}\int_0^T \frac{|d\langle O(t)\rangle|}{\Delta O(t)}. \tag{18}$$

Therefore, we have

$$T \geqslant T^{O}_{\mathrm{SQSL}} \geqslant T^{O}_{\mathrm{QSL}}. \tag{19}$$

This shows that indeed SQSLO is tighter than QSLO.

IV. STRONGER QSL FOR STATES AND ENTANGLEMENT CAPACITY

In this section, we delve into the relationship between SQSL for observables and SQSL concerning states. Notably, SQSL for state emerges as a distinctive instance within the broader framework of SQSL for observable, when we consider the observable as the projector of the initial state. For realizing that, let us consider a quantum system with an initial state $|\Psi\rangle = \sum_i c_i|i\rangle$. We continue with the observable taking the form of a projector, i.e., $O(0) = P$. Consequently, the probability of finding the system in state $|i\rangle$ at time $t = 0$ becomes $|c_i|^2$, upon performing measurement with projector defined as $P = |i\rangle\langle i|$. Now we wish to study the bound on speed limit for the projector for the quantum system evolving a state $|i\rangle$ unitarily in time. Using Eq. (17) in an alternative way, we can express the quantum speed limit for the projector as given by

$$T \geqslant \frac{\hbar\ \Lambda(T)}{2\Delta H}\int_0^T \frac{|d\langle P(t)\rangle|}{\Delta P(t)}, \tag{20}$$

where $P(t) = U(t)P(0)U(t)^{\dagger}$ and $\langle P(t)\rangle = p(t)$ is the probability of the quantum system in state $|i\rangle$ at some later time t.

The above bound can be expressed as

$$T \geqslant \frac{\hbar\Lambda(T)}{\Delta H}|\arcsin[\sqrt{p(T)}] - \arcsin[\sqrt{p(0)}]|, \tag{21}$$

where $\Lambda(T) = \frac{1}{1-\overline{R}(t)}$, with $\overline{R}(t) = \frac{1}{T}\int_0^T R(t)\ dt$. Now if we choose $p(0) = 1$, i.e., $|\Psi\rangle = |i\rangle$, then the above inequality results in the following bound:

$$T \geqslant \frac{\hbar\Lambda(T)}{\Delta H}\arccos[\sqrt{p(T)}]. \tag{22}$$

This is equivalent to the stronger speed limit for the state obtained in Ref. [47]. As we know the Mandelstam and Tamm bound is a special case of the stronger speed limit for the state, we can say that the stronger speed limit for the state and MT bound, both are special cases of the stronger quantum speed limit for the observable. Thus, our result unifies the previous known bounds on the observable and state. Next, we apply the SQSL for state to provide stronger bound for the entanglement rate using capacity of entanglement.

Improved bounds on rate of entanglement through capacity of entanglement using SQSL for states

The dynamics of entanglement under two-qubit nonlocal Hamiltonian has been addressed in Ref. [99]. Further, the inquiry on capacity of entanglement for two-qubit nonlocal Hamiltonian and its properties have been addressed in Ref. [51]. It was discovered that the defined capacity of entanglement indeed played a role in giving parameter free bound to quantum speed limit for creating entanglement. In this section, we address the following question: Can we improve upon the

quantum speed limit bound, using the stronger uncertainty relation? As we will see, indeed one can get a tighter bound in such case and it again bolsters the point that the capacity of entanglement has a physical meaning in deciding how much time a bipartite state takes in order to produce a certain amount of entanglement.

Let us briefly discuss about the two-qubit system, for which the nonlocal Hamiltonian can be expressed as (except for trivial constants)

$$H = \vec{\alpha}\cdot\vec{\sigma}^A \otimes \mathcal{I}_B + \mathcal{I}_A \otimes \vec{\beta}\cdot\vec{\sigma}^B + \sum_{i,j=1}^{3} \gamma_{ij}\sigma_i^A \otimes \sigma_j^B, \quad (23)$$

where $\vec{\alpha}, \vec{\beta}$ are real vectors, γ is a real matrix and, $\mathcal{I}_A$ and $\mathcal{I}_B$ are identity operator acting on $\mathcal{H}_A$ and $\mathcal{H}_B$. The above Hamiltonian can be rewritten in one of the two canonical forms under the action of local unitaries acting on each qubits [99,100]. This is given by

$$H^{\pm} = \mu_1\sigma_1^A \otimes \sigma_1^B \pm \mu_2\sigma_2^A \otimes \sigma_2^B + \mu_3\sigma_3^A \otimes \sigma_3^B, \quad (24)$$

where $\mu_1 \geqslant \mu_2 \geqslant \mu_3 \geqslant 0$ are the singular values of matrix γ [99]. Using the Schmidt decomposition, any two-qubit pure state can be written as

$$|\Psi\rangle_{AB} = \sqrt{p}\,|\phi\rangle\,|\chi\rangle + \sqrt{1-p}\,|\phi^{\perp}\rangle\,|\chi^{\perp}\rangle\,. \quad (25)$$

We can utilize the form of Hamiltonian in Eq. (24) and choose H^+ [i.e., assuming $\det(\gamma) \geqslant 0$] to evolve the state in Eq. (25) without losing any generality [99]. To further showcase a specific example, let us choose $|\phi\rangle = |0\rangle$ and $|\chi\rangle = |0\rangle$. Thus, the state at time $t = 0$ takes the form

$$|\Psi(0)\rangle_{AB} = \sqrt{p}\,|0\rangle\,|0\rangle + \sqrt{1-p}\,|1\rangle\,|1\rangle\,. \quad (26)$$

Under the action of the nonlocal Hamiltonian, the joint state at time t can be written as ($\hbar = 1$)

$$|\Psi(t)\rangle_{AB} = e^{-iHt}\,|\Psi\rangle_{AB} = \alpha(t)\,|0\rangle\,|0\rangle + \beta(t)\,|1\rangle\,|1\rangle\,, \quad (27)$$

where $\alpha(t) = e^{-i\mu_3 t}[\sqrt{p}\cos(\theta t) - i\sqrt{1-p}\sin(\theta t)]$, $\beta(t) = e^{-i\mu_3 t}[\sqrt{1-p}\cos(\theta t) - i\sqrt{p}\sin(\theta t)]$, and $\theta = (\mu_1 - \mu_2)$. To evaluate the capacity of entanglement, we would require the reduced density matrix of the two-qubit evolved state, $\rho_A(t) = \mathrm{tr}_B[\rho_{AB}(t)]$, which is given by

$$\rho_A(t) = \lambda_1(t)\,|0\rangle\,\langle 0| + \lambda_2(t)\,|1\rangle\,\langle 1|\,, \quad (28)$$

where $\lambda_1(t) = |\alpha(t)^2|$ and $\lambda_2(t) = |\beta(t)^2|$, thus read as

$$\lambda_1(t) = \tfrac{1}{2}[1 - (1-2p)\cos(2\theta t)],$$
$$\lambda_2(t) = \tfrac{1}{2}[1 + (1-2p)\cos(2\theta t)].$$

The capacity of entanglement at a later time t can be calculated from the variance of modular Hamiltonian K_A defined as $K_A = -\log_2\rho_A$. This is given by

$$C_{\mathrm{E}}(t) = \mathrm{tr}\{\rho_A(t)[-\log_2\rho_A(t)]^2\} - \{\mathrm{tr}[-\rho_A(t)\log_2\rho_A(t)]\}^2,$$
$$= \sum_{i=1}^{2}\lambda_i(t)\log_2^2\lambda_i(t) - \left(-\sum_{i=1}^{2}\lambda_i(t)\log_2\lambda_i(t)\right)^2. \quad (29)$$

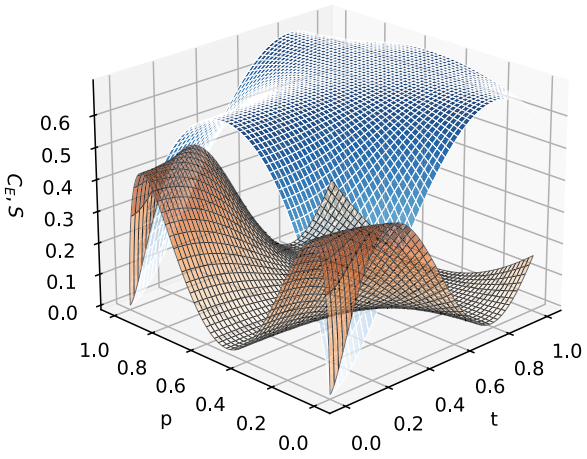

FIG. 1. Surface plot for capacity of entanglement $C_{\mathrm{E}}(p,t)$ (darker orange surface plot) and entanglement entropy $S_{\mathrm{EE}}(p,t)$ (lighter blue surface plot) vs p and t taking $\theta = 1$

Further for Eq. (27), one can evaluate the entanglement entropy and capacity as:

$$C_{\mathrm{E}}(t) = -\frac{1}{2}\mathrm{Tanh}^{-1}[(2p-1)\cos(2\theta t)]^2 \times [-1 + 4p(p-1) + (1-2p)^2\cos(4\theta t)]$$

$$S_{\mathrm{EE}} = \frac{e^{-2it\theta}}{4}\Bigg[[-1 - 2e^{2it\theta} + 2p + e^{4it\theta}(-1+2p)] \times \log_2\left[\frac{1 + (1-2p)\cos(2t\theta)}{2}\right] - [-1 + 2e^{2it\theta} + 2p + e^{4it\theta}(-1+2p)] \times \log_2\left[\frac{1 - (1-2p)\cos(2t\theta)}{2}\right]\Bigg] \quad (30)$$

for chosen parameters p and θ. The plot in Fig. 1 shows how entanglement entropy and capacity of entanglement varies for some chosen value of $\theta = 1$, where capacity reduces to zero for when the state is either separable or stationary [51,99].

Now, for evaluating bound on the rate of entanglement, we use the stronger-uncertainty relation in the form of Eq. (12) for the two noncommuting operators $K_{AB} = K_A \otimes \mathcal{I}$ and H_{AB}. This leads to

$$\tfrac{1}{2}|\langle\Psi(t)|[K_A \otimes \mathcal{I}, H_{AB}]|\Psi(t)\rangle| \leqslant \Delta K_A\ \Delta H_{AB}\ [1 - R(t)]. \quad (31)$$

Using Eq. (14) (for $O = K_A$) in Eq. (31), we then obtain

$$\frac{\hbar}{2}\left|\frac{\mathrm{d}\langle K_A\rangle}{\mathrm{d}t}\right| \leqslant \Delta K_A\ \Delta H_{AB}\ [1 - R(t)]. \quad (32)$$

Let $\Gamma(t)$ denote the rate of entanglement. Recall that the average of the modular Hamiltonian is the entanglement entropy S_{EE}. In terms of the entanglement rate $\Gamma(t)$, the above equation can be written as

$$|\Gamma(t)| \leqslant \frac{2}{\hbar}\Delta K_A\ \Delta H_{AB}\ [1 - R(t)]. \quad (33)$$

Since the square of the standard deviation of modular Hamiltonian is the capacity of entanglement, so in terms of the capacity of entanglement, we can write above bound as

$$|\Gamma(t)| \leqslant \frac{2}{\hbar}\sqrt{C_{\rm E}(t)}\ \Delta H_{AB}\ [1 - R(t)]. \tag{34}$$

We can interpret the above formula by noting that one can define the speed of transportation of bipartite pure entangled state on projective Hilbert space of the given system by the expression $\frac{2}{\hbar}\Delta H_{AB}$. Further using the Fubini-Study metric for two nearby states, one can define the infinitesimal distance between two nearby states [2,8,101] as

$$\mathrm{d}S^2 = 4(1 - |\langle\Psi(t)\,|\Psi(t + \mathrm{d}t)\rangle|^2) = \frac{4}{\hbar^2}\Delta H_{AB}^2\ \mathrm{d}t^2. \tag{35}$$

Therefore, the speed of transportation as measured by the Fubini-Study metric is given by $V = \frac{\mathrm{d}S}{\mathrm{d}t} = \frac{2}{\hbar}\Delta H_{AB}$. Thus, the entanglement rate is upper bounded by the speed of quantum evolution [37] and the square root of the capacity of entanglement and correction factor due to stronger uncertainty, i.e., $|\Gamma(t)| \leqslant \sqrt{C_{\rm E}(t)}\ V\ [1 - R(t)]$.

We know from Ref. [102] that for an ancilla unassisted case, the entanglement rate is upper bounded by $c\|H\|\log_2 d$, where $d = \min(\dim\mathcal{H}_A, \dim\mathcal{H}_B)$, c being a constant between the value 1 and 2, and $\|H\|$ is operator norm of Hamiltonian, which corresponds to $p = \infty$ of the Schatten p norm of H, which is defined as $\|H\|_p = [\mathrm{tr}(\sqrt{H^{+}H})^p]^{\frac{1}{p}}$. Now, using the fact that the maximum value of capacity of entanglement is proportional to $S_{\max}(\rho_A)^2$ [50], where $S_{\max}(\rho_A)$ is maximum value of von Neumann entropy of subsystem, which is upper bounded by $\log_2 d_A$, where d_A is the dimension of Hilbert space of subsystem A, and $\Delta H \leqslant \|H\|$, a similar bound on the entanglement rate can be obtained from Eq. (34). Further the factor $[1 - R(t)]$ varies between 0 and 1 for given standard choice of Eq. (27). Thus, the bound on the entanglement rate given in Eq. (34) is significantly stronger than the previously known bound and will be shown subsequently to be a improvement upon the bound found in Ref. [51].

This bound on entanglement rate can be used to provide QSL, which decides how fast a quantum state evolves in time from an initial state to a final state [103]. Since the original bound was given by Mandelstam and Tamm, over the past decade there have been active explorations on generalizing the notion of QSL to mixed states [35,104] and on resources that a quantum system might posses [105]. The notion of generalized quantum speed limit has been explored in Ref. [106]. Further, the quantum speed limit for observables has been defined and it was shown that the QSL for state evolution is a special case of the QSL for observable [47]. For a quantum system evolving under a given dynamics, there exists a fundamental limitation on the speed for entropy $S(\rho)$, maximal information $I(\rho)$, and quantum coherence $C(\rho)$ [107] as well as on other quantum correlations such as entanglement, quantum mutual information, and Bell-CHSH correlation [97].

Now, we are in the position to give a stronger uncertainty based expression for QSL bound,

$$\int_0^T \left|\frac{\mathrm{d}S_{\rm EE}(t)}{\mathrm{d}t}\right|\mathrm{d}t \leqslant \int_0^T \frac{2}{\hbar}\sqrt{C_{\rm E}(t)}\ \Delta H\ [1 - R(t)]\ \mathrm{d}t. \tag{36}$$

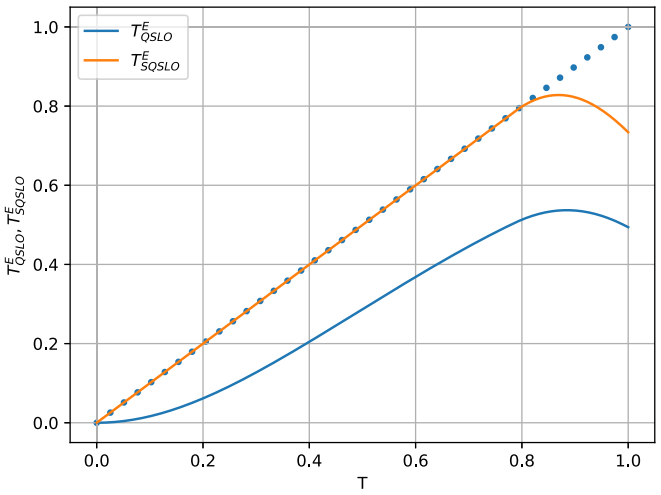

FIG. 2. Here we depict $T^E_{\rm QSLO}$ (top line), $T^E_{\rm SQSLO}$ (bottom curve) vs T with $p = 0.1$ for $\theta = 1.0$.

For the time-independent Hamiltonian, we obtain the following bound for the stronger quantum speed limit for entanglement:

$$T \geqslant T^E_{\rm SQSLO} := \frac{\hbar|S_{\rm EE}(T) - S_{\rm EE}(0)|}{2\Delta H\frac{1}{T}\int_0^T \sqrt{C_{\rm E}(t)}\ [1 - R(t)]\mathrm{d}t}. \tag{37}$$

It is thus clear that evolution speed for entanglement generation (or degradation) is a function of capacity of entanglement $C_{\rm E}$ and a correction factor due to stronger uncertainty relation. Thus, we can say that $C_{\rm E}$ with $[1 - R(t)]$ together controls how much time a system may take to produce a certain amount of entanglement. Extending the analysis of the bound, we have calculated $R(t)$ by using the above-prescribed expression. We note that under certain choice of $|\psi^{\perp}\rangle$ this corresponds to the system evolving along the geodesic path [46]. The corresponding choice is as

$$|\psi^{\perp}(t)\rangle = \frac{O(t) - \langle O(t)\rangle}{\Delta O(t)}|\psi(t)\rangle, \tag{38}$$

and with this, the speed limit bound is the most optimized.

To examine the tightness of the given QSL bound for generation of entanglement by taking an example of the state as given in Eq. (27) for which we have estimated both capacity of entanglement $C_{\rm E}$ and entanglement entropy $S_{\rm EE}$ in Eq. (30). Further with $\Delta H = |\theta\ (1 - 2p)|$ and evaluating $R(t)$ as defined in Eq. (13) making use of $|\Psi^{\perp}(t)\rangle$ through Eq. (38) we plot for $T^E_{\rm SQSLO}$ and $T^E_{\rm QSLO}$ vs $T \in [0, 1]$ in Fig. 2 where $T^E_{\rm QSLO}$ is given as [51]

$$T \geqslant T^E_{\rm QSLO} := \frac{\hbar|S_{\rm EE}(T) - S_{\rm EE}(0)|}{2\Delta H\frac{1}{T}\int_0^T \sqrt{C_{\rm E}(t)}\mathrm{d}t}. \tag{39}$$

We clearly see that the operator stronger quantum speed limit $T^E_{\rm SQSLO}$, which is with the correction factor gives a significantly tighter bound than the other $T^E_{\rm QSLO}$. With the choice of state and Hamiltonian with $p = 0.1$ and $\theta = 1.0$, we indeed show that the bound is tighter and achievable. Further, in Fig. 3, we plot $T^E_{\rm SQSLO}$ vs T for a fixed p but several θ values, which shows that we get better bounds for lower values of θ

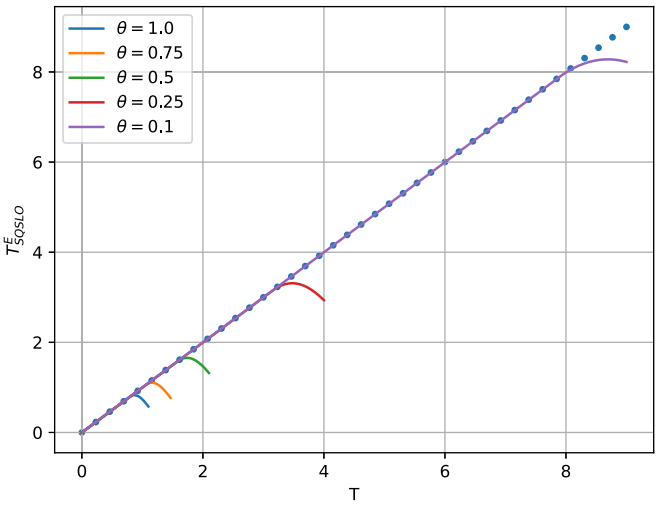

FIG. 3. Speed limit plot for entanglement generation for varying θ keeping $p = 0.1$ fixed where tight bound for longest time could be achieved for lowest $\theta = 0.1$ and shortest for largest $\theta = 1.0$.

and each of this case, T^E_{SQSLO} gives a tighter bound. In the subsequent section, we demonstrate that one obtains better bounds through SQSLO compared to QSLO by illustrating through two important examples.

V. ILLUSTRATIONS AND EXAMPLES

A. Improved bounds on modular energy using SQSLO

In the previous section, we have explored the study of entanglement generation using SQSL for state. Here, we would like to investigate how the modular Hamiltonian itself changes under unitary transformation in the Heisenberg picture. Consider a two-qubit system with a similar generalized canonical forms of nonlocal Hamiltonian $H^{\pm}$ as in Eq. (24). Further our state in this case retains the form $|\Psi\rangle_{AB} = |\Psi(0)\rangle_{AB}$ as in Eq. (26). As such the state operator of the composite system also retains its form as

$$\rho_{AB} = \rho_{AB}(0) = |\Psi(0)\rangle_{AB}\langle\Psi(0)|. \tag{40}$$

We again choose H^+ form of canonical Hamiltonian to time evolve the following composite modular Hamiltonian:

$$K_{AB} \equiv K_{AB}(0) = K_A \otimes \mathcal{I}_B, \tag{41}$$

where $K_A \equiv K_A(0) = -\log_2 \rho_A$ is the modular Hamiltonian and $\rho_A(0) = \mathrm{tr}_B[\rho_{AB}(0)]$. In the Heisenberg picture, the operator of the composite AB system evolves with unitary operator $U(t) = e^{-iH^+t}$

$$K_{AB}(t) = U^{\dagger}(t)K_{AB}(0)U(t). \tag{42}$$

We interpret the quantity $\langle K_{AB}(t)\rangle = \mathrm{tr}(\rho_{AB}\, K_{AB}(t))$ as the modular energy $\mathcal{E}_{\mathcal{M}}$ in the Heisenberg picture. Note that even though $\langle K_{AB}(0)\rangle = \mathrm{tr}[\rho_A(0)K_A(0)]$ represents entanglement at $t = 0$, $K_{AB}(t)$ does not represent entanglement at time t in the Heisenberg picture.

Now, the variance of composite modular Hamiltonian $\mathcal{C}_{\mathcal{M}}$ can be written as

$$\mathcal{C}_{\mathcal{M}}(t) = \Delta K_{AB}(t)^2 = \langle K^2_{AB}(t)\rangle - \langle K_{AB}(t)\rangle^2. \tag{43}$$

The generalized expression for the $\mathcal{E}_{\mathcal{M}}$ and $\mathcal{C}_{\mathcal{M}}$ can be evaluated and expressed as

$$\begin{aligned}\mathcal{C}_{\mathcal{M}}(t) &= \frac{1}{4}\log_2\left(-1+\frac{1}{p}\right)^2 (4p(1-p)\,\cos(2\theta t)^2 \\ &\quad + \sin(2\theta t)^2) \\ \mathcal{E}_{\mathcal{M}}(t) &= -(1-2p)\,\mathrm{arctanh}(1-2p)\,\cos(2\theta t) \\ &\quad - \frac{1}{2}\log_2[p(1-p)].\end{aligned} \tag{44}$$

We begin by making use of stronger-uncertainty relation for the case of in general noncommuting Hamiltonians $K_{AB}(t)$ and H_{AB} and derive SQSLO bound for modular energy. Denoting $|\Psi\rangle_{AB} = |\Psi\rangle$ for brevity, we have

$$\tfrac{1}{2}|\langle\Psi|[K_{AB}(t), H_{AB}]|\Psi\rangle| \leqslant \Delta K_{AB}\Delta H_{AB}[1 - R(t)], \tag{45}$$

which leads to

$$\frac{\hbar}{2}\left|\frac{\mathrm{d}\langle K_{AB}(t)\rangle}{\mathrm{d}t}\right| = \frac{\hbar}{2}\left|\frac{\mathrm{d}\mathcal{E}_M}{\mathrm{d}t}\right| \leqslant \Delta K_{AB}(t)\Delta H_{AB}[1 - R(t)]. \tag{46}$$

As $\Delta K_{AB}(t) = \sqrt{\mathcal{C}_M(t)}$, from Eq. (43), we get

$$\left|\frac{\mathrm{d}\mathcal{E}_M}{\mathrm{d}t}\right| \leqslant \frac{2}{\hbar}\sqrt{\mathcal{C}_M(t)}\Delta H_{AB}[1 - R(t)]. \tag{47}$$

This is a bound on the rate of the modular energy in the Heisenberg picture. This is clearly distinct from the earlier case in the Schrödinger picture (as these two quantities are different).

For the purpose of evaluating $R(t)$, we will need the optimized $|\Psi^{\perp}\rangle$ as prescribed in Eq. (38). It is important to mention that though the state vector of the system $|\Psi\rangle$ remains time independent in the considered picture, yet $|\Psi^{\perp}\rangle$ carries an explicit time dependence due to the prescription used involving operators that are time evolving themselves. So at each instant of time of the operator evaluation, it picks up a different $|\Psi^{\perp}\rangle$ while only maintaining that it be perpendicular to the taken choice of $|\Psi\rangle$. It goes without saying that such $|\Psi^{\perp}\rangle$ is not physically relevant to the system, as it plays no role in the description of it at any point in time. The general expression for this choice evaluates out as given in Appendix A (A3). Now this leads us to the following SQSLO bound as given by

$$T \geqslant T^{\mathcal{M}}_{\mathrm{SQSLO}} := \frac{\hbar}{2\,\Delta H_{AB}}\int_0^T \frac{|\mathrm{d}\mathcal{E}_M|}{\sqrt{\mathcal{C}_M(t)}\,[1 - R(t)]}. \tag{48}$$

We get the equivalent $T^{\mathcal{M}}_{\mathrm{QSLO}}$ case from the Robertson-Schrödinger uncertainty relation, which is akin to dropping the correction factor from Eq. (48)

$$T \geqslant T^{\mathcal{M}}_{\mathrm{QSLO}} := \frac{\hbar}{2\,\Delta H_{AB}}\int_0^T \frac{|\mathrm{d}\mathcal{E}_M|}{\sqrt{\mathcal{C}_M(t)}}. \tag{49}$$

Now, with $\Delta H_{AB} = |(1-2p)\,\theta|$, we plot SQSLO and QSLO bounds in Fig. 4 for the case of $p = 0.1$ and $\theta = 1.0$ for which $R(t)$ is given in Eq. (A4). We observe that in the case of Heisenberg picture, the QSLO bound, i.e., $T^{\mathcal{M}}_{\mathrm{QSLO}}$ turns out to be a bit loose whereas the SQSLO bound, i.e., $T^{\mathcal{M}}_{\mathrm{SQSLO}}$, which is with the correction factor turns out to be saturated.

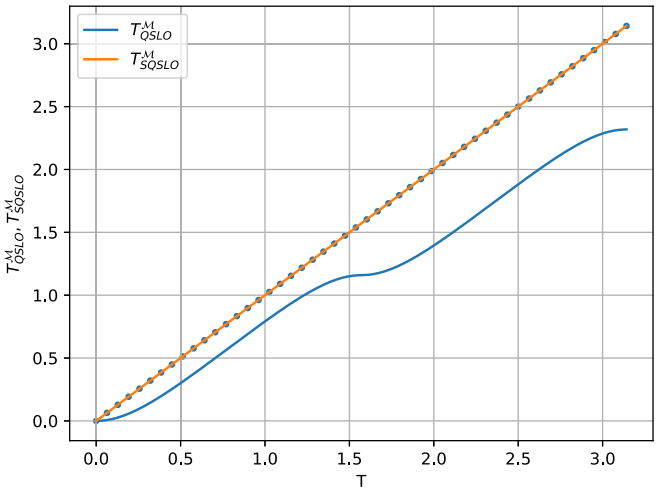

FIG. 4. Here we depict $T^{\mathcal{M}}_{\mathrm{QSLO}}$ (bottom curve), $T^{\mathcal{M}}_{\mathrm{SQSLO}}$ (top saturated line) vs T with $p = 0.1$ for $\theta = 1.0$.

We further plot QSLO bound for four cases of $p = \{0.1, 0.4\}$ and $\theta = \{0.5, 1.0\}$ cases using expressions for respective $R(t)$ from Eqs. (A4)–(A7), which is shown in Fig. 5. We observe and can conclude from the figure upon plotting with several example cases, that the $T^{\mathcal{M}}_{\mathrm{QSLO}}$ bound is not optimal.

Upon plotting for $T^{\mathcal{M}}_{\mathrm{QSLO}}$ and $T^{\mathcal{M}}_{\mathrm{SQSLO}}$ bounds for varying $\theta = \{0.5, 1.0\}$ and fixed $p = 0.1$ cases in Fig. 6. We observe that the SQSLO bound turns out to be saturated for any choice in parameters. This shows that the SQSLO for the rate of modular Hamiltonian is tight and saturated.

B. Improved bounds on charging time of quantum batteries through SQSLO

The models of quantum engines and refrigerators have been of great interest lately as they help in simulating theoretical efforts to formulate fundamental thermodynamical principles and bounds, which are valid on micro or nanoscale. It has been found that these can differ from the standard

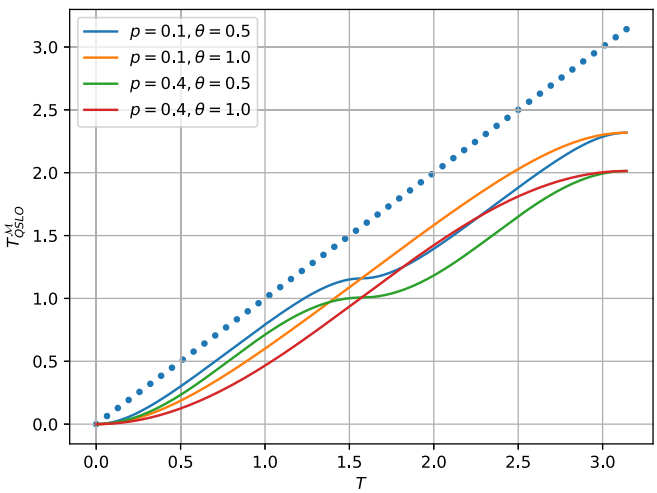

FIG. 5. Depiction of $T^{\mathcal{M}}_{\mathrm{QSLO}}$ for chosen values of p and θ. The dotted line is the reference ideal (saturated) case.

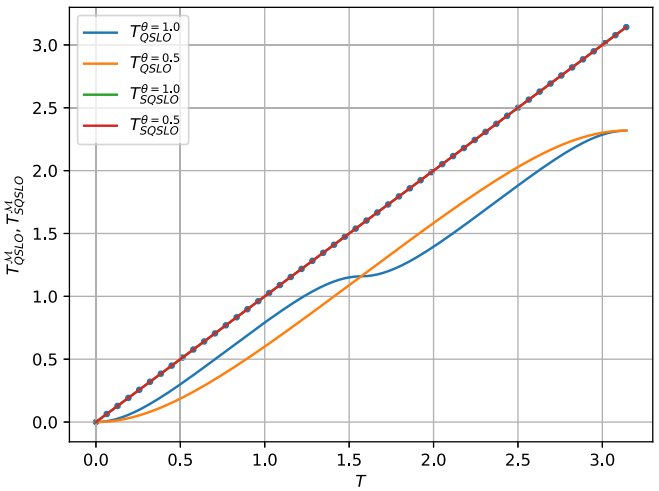

FIG. 6. Depiction of $T^{\mathcal{M}}_{\mathrm{QSLO}}$ (curves) and $T^{\mathcal{M}}_{\mathrm{SQSLO}}$ (overlap with reference saturation case) for fixed $p = 0.1$ and varying θ. We observe that $T^{\mathcal{M}}_{\mathrm{QSLO}}$ for $\theta = 0.5$ takes lead over $T^{\mathcal{M}}_{\mathrm{QSLO}}$ for $\theta = 1.0$ after $T = \pi/2$.

ones and converge only in the limit of macroscopic systems [108]. The amount of work that can be extracted from a small quantum mechanical system that is used to temporarily store energy and to transfer it from a production to a consumption center is the main content of a quantum battery. It is not coupled to external thermal baths in order to drive thermodynamical engines, but rather its dynamics is controlled by external time-dependent fields.

The battery comes with its initial state ρ and an internal Hamiltonian H_B. The process of energy extraction then follows when this system is reversibly evolved under some fields that are turned on during time interval $[0, T]$. The maximal amount of work that can be extracted by such a process has been explored in Ref. [54]. Subsequently, numerous researchers have dedicated their efforts to furthering the understanding and exploitation of nonclassical features of quantum batteries such as in Ref. [82]. In many-body quantum systems characterized by multiple degrees of freedom, the presence of quantum batteries, capable of storing or releasing energy, is ubiquitous. In this section, we aim to determine the minimum achievable unitary charging time of the quantum battery utilizing the discussed SQSLO bound.

Consider a scenario where a quantum battery, with energy denoted by the Hamiltonian H_B, interacts with an external charging field represented by H_C. Consequently, the total energy of the system is determined by the combined Hamiltonian, expressed as follows:

$$H_T = H_B + H_C. \tag{50}$$

Now, the ergotropy is defined as the quantum system's capacity to extract energy via unitary operations from the quantum battery [109], and is expressed as

$$\mathcal{E}(t) = \langle\Psi(t)|H_B|\Psi(t)\rangle - \langle\Psi(0)|H_B|\Psi(0)\rangle, \tag{51}$$

where $|\Psi(t)\rangle$ and $|\Psi(0)\rangle$ are the final and initial state of the given quantum system.

While the aforementioned expression holds true in the Schrödinger picture, we would now like to switch over to

its study in the Heisenberg picture where the expression for ergotropy takes the form

$$\mathcal{E}(t) = \langle\Psi(0)|[H_B(t) - H_B(0)]|\Psi(0)\rangle, \tag{52}$$

where $H_B(t) = e^{\frac{iHt}{\hbar}} H_B(0) e^{-\frac{iHt}{\hbar}}$ and $H_B(0) = H_B$.

The rate of change of ergotropy of quantum battery during the charging process can be obtained as

$$\frac{d\mathcal{E}(t)}{dt} = \frac{d}{dt}\langle\Psi(0)|H_B(t)|\Psi(0)\rangle. \tag{53}$$

Using our bound we can write SQSLO for the ergotropy as

$$T \geqslant \frac{\hbar}{2\Delta H_T}\int_0^T \frac{|d\mathcal{E}(t)|}{\Delta H_B(t)[1 - R(t)]}, \tag{54}$$

where $R(t) = \frac{1}{2}|\langle\Psi^{\perp}|\frac{H_B(t)}{\Delta H_B(t)} \mp i\frac{H_T}{\Delta H_T}|\Psi\rangle|^2$ and T is the charging time period of the quantum battery.

This SQSLO for QBs can also be reexpressed as:

$$T^{QB}_{\text{SQSLO}} = \frac{\hbar T}{2\Delta H_T}\left\langle\!\!\left\langle \frac{|\mathcal{E}(T) - \mathcal{E}(0)|}{\Delta H_B(t)(1 - R(t))}\right\rangle\!\!\right\rangle_T, \tag{55}$$

where $\langle\langle A(t)\rangle\rangle_T = \frac{1}{T}\int_0^T \mathrm{d}t\, A(t)$, is the time average of the quantity $A(t)$.

Now that we have derived the quantum speed limit (QSL) formula for quantum batteries (QB's) in a general case, let us take up a specific example where we apply our SQSLO bound on QB's. Our chosen example involves an entanglement-based QB consisting of two qubit cells and two coupled two-level systems. To charge the QB effectively, we must individually couple each cell with local fields. Consequently, our total Hamiltonian H_T can be expressed as given in Ref. [82]

$$H_T = H_B + H_C + H_{\text{int}}, \tag{56}$$

where $H_B = \hbar\omega_0 \sum_{n=1}^{2} \sigma_n^z$ being the battery Hamiltonian. Here, ω_0 is the identical Larmor frequency for both the qubits. Let us label $|\uparrow\rangle$ and $|\downarrow\rangle$ as ground and excited states for a single qubit. With this one can define the fully charged state of the battery as $|\text{full}\rangle = |\uparrow\uparrow\rangle$ with full energy $E_{\text{full}} = 2\hbar\omega$, and empty one as $|\text{emp}\rangle = |\downarrow\downarrow\rangle$ with low energy $E_{\text{emp}} = -2\hbar\omega$. Hence, the maximum energy that can be stored in the battery reads $\mathcal{E}_{\max} = 4\hbar\omega$.

We consider the driving Hamiltonian to be comprised of two parts, having charging part $H_C = \hbar\Omega\sum_{n=1}^{2}\sigma_n^x$ and nearest-neighbor interaction part $H_{\text{int}} = \hbar J(\sigma_1^x\sigma_2^x + \sigma_1^y\sigma_2^y + \sigma_1^z\sigma_2^z)$, where J is the strength of two-body interaction. The most general state of two qubits then reads as

$$|\Psi(0)\rangle = \mu\,|\uparrow\uparrow\rangle + \nu\,|\uparrow\downarrow\rangle + \eta\,|\downarrow\uparrow\rangle + \delta\,|\downarrow\downarrow\rangle\,. \tag{57}$$

Let us consider the case for the most general two-qubit nonentangled state with,

$$\begin{aligned}
\mu &= \sin(\theta_1)\sin(\theta_2)e^{i(\varphi_1+\varphi_2)}\\
\nu &= \sin(\theta_1)\cos(\theta_2)e^{i\varphi_1}\\
\eta &= \cos(\theta_1)\sin(\theta_2)e^{i\varphi_2}\\
\delta &= \cos(\theta_1)\cos(\theta_2),
\end{aligned} \tag{58}$$

where $\theta_1, \theta_2 \in [0, \pi]$ and $\varphi_1, \varphi_2 \in [0, 2\pi]$. For the purpose of illustration, let us assume that at the beginning of the charging process, the battery is assumed to be empty, i.e., $\rho(0) = |\text{emp}\rangle\langle\text{emp}|$, which is achieved when we put $\theta_1 = \theta_2 = 0$ in Eq. (58).

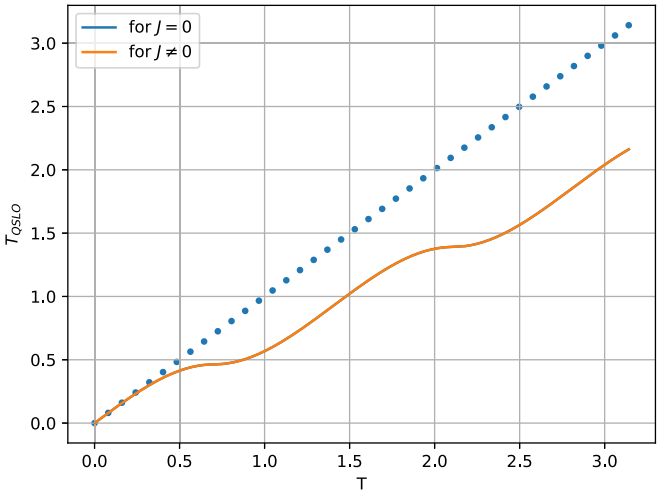

FIG. 7. Figure shows that the QSLO bound plots (curves) for both parallel ($J = 0$) and collective ($J \neq 0$) quantum battery scenarios overlap. The dotted curve is the reference ideal case.

The ergotropy Eq. (52) in this case under Heisenberg picture upon evaluation reads as

$$\mathcal{E}(t) = \frac{4\omega\Omega^2}{\omega^2 + \Omega^2}\sin(\sqrt{\omega^2 + \Omega^2}\,t)^2. \tag{59}$$

We would like to study the bounds on the charging time for mentioned scenario above. First we look at the QSLO bound studied in previous section, with a similar form to Eq. (49) for quantum batteries as

$$T_{\text{QSLO}} = \frac{\hbar}{2\Delta H_T}\int_0^T \frac{|d\mathcal{E}(t)|}{\Delta H_B(t)}, \tag{60}$$

where ΔH_T and $\Delta H_B(t)$ can be evaluated for chosen values of parameters ω, Ω, and J in above bound.

With our general Hamiltonian for QB defined as above, let us take a case of parallel charging when $J = 0$, rendering the interaction Hamiltonian inactive. Similarly, we can determine the QSLO for the case of collective charging when $J \neq 0$ using Eq. (60). Upon plotting these two speed limit functions, as depicted in Fig. 7, we observe that for the above two cases, the QSLO bound overlaps. Over that, there is a clear deviation from the reference ideal case, i.e., $T_{\text{QSLO}} = T$. It thus leaves the ground for improvement. This observation holds true for both scenarios of the QB Hamiltonian, namely the parallel and collective charging cases. Hence, we would like to compute the bounds by applying the SQSLO bound to both the cases.

Next, we study the scenarios involving coupled and decoupled cases. When $J = \Omega$, we say the system is coupled, whereas for $J \neq \Omega$, it represents the decoupled scenario. To compute the QSLO for both the coupled and decoupled Hamiltonians, we follow a similar procedure as we did for the parallel and collective QB cases. A novel aspect of our approach is the application of the SQSLO in both the coupled and decoupled Hamiltonians. The expression for the SQSLO

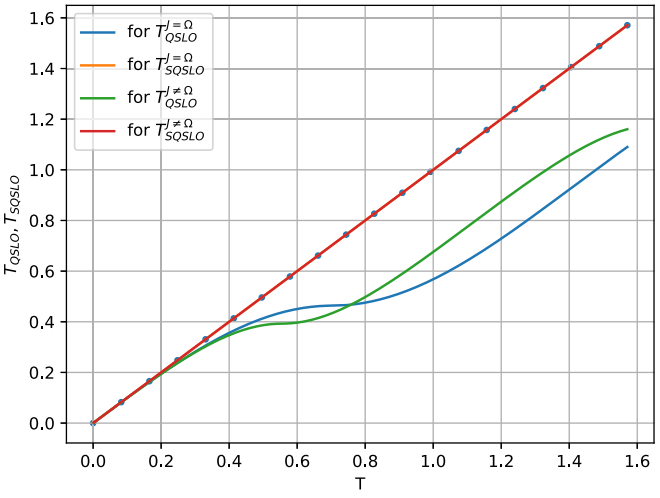

FIG. 8. Figure depicts plots for both QSLO and SQSLO bounds for both coupling ($J = \Omega$) and decoupling ($J \neq \Omega$) quantum battery scenarios. The QSLO bounds overlap with reference ideal (saturated) case, whereas for QSLO curves, decoupling case takes the lead close to after $T = 0.8$.

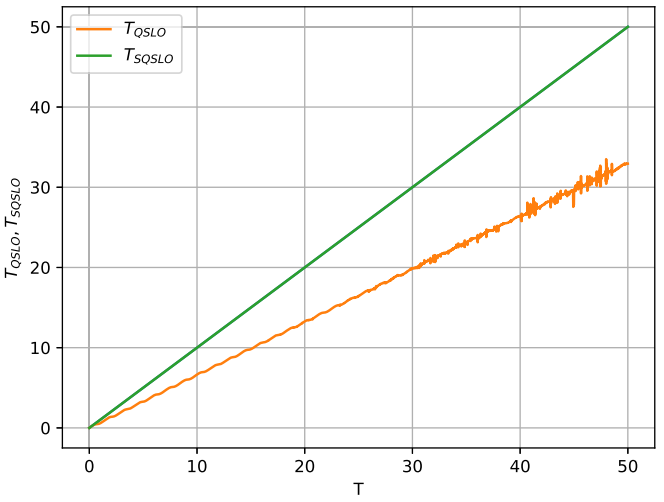

FIG. 9. Figure shows the long time behavior of T_{QSLO} (bottom unsaturated curve), T_{SQSLO} (tight and saturated overlap with reference ideal line).

bound is given as

$$T_{\mathrm{SQSLO}} = \frac{\hbar}{2\Delta H_T}\int_0^T \frac{|d\mathcal{E}(t)|}{\Delta H_B(t)[1-R(t)]}, \tag{61}$$

where for the coupled case (with $J = \Omega = 1$ and $\omega = 2$) we obtain expression of $R(t)$ as

$$R(t) = \frac{1}{2}\left(\begin{cases} 2 - \frac{2\sqrt{10}\cos(\sqrt{5}t)}{\sqrt{9+\cos(2\sqrt{5}t)}} & \sin(\sqrt{5}t) < 0 \\ 2 + \frac{2\sqrt{10}\cos(\sqrt{5}t)}{\sqrt{9+\cos(2\sqrt{5}t)}} & \text{True,} \end{cases}\right), \tag{62}$$

where $|\Psi\rangle$ and $|\Psi^{\perp}\rangle$ are given in Appendix B. For the purpose of evaluating $R(t)$, we need the optimized $|\Psi^{\perp}\rangle$ as prescribed in Eq. (38).

Again, for the decoupled case, i.e., $J \neq \Omega$ (taking $J = 1,\ \Omega = 4,\ \omega = 2$) we evaluate the bound using the expression for bound in Eq. (61). The expression of $R(t)$ upon evaluation comes as

$$R(t) = \frac{1}{2}\left(\begin{cases} 2 - \frac{4\cos(2\sqrt{2}t)}{\sqrt{3+\cos(4\sqrt{2}t)}} & \sin(2\sqrt{2}t) < 0 \\ 2 + \frac{4\cos(2\sqrt{2}t)}{\sqrt{3+\cos(4\sqrt{2}t)}} & \text{True,} \end{cases}\right), \tag{63}$$

where $|\Psi\rangle$ and $|\Psi^{\perp}\rangle$ are given in Appendix B.

We have depicted both SQSLO curves for both the coupling and decoupling cases. Surprisingly, in both scenarios, the SQSLO plots exhibit remarkable accuracy as they overlap while showing saturation, as can be seen in Fig. 8. As expected, QSLO does not yield optimally tight bounds for both coupling and decoupling cases as shown in the same figure. From these plots, we can conclude that SQSLO performs remarkably well, accurately representing the speed limit behavior in QB systems for both coupling and decoupling cases. This result is quite a significant improvement upon earlier bounds and is the optimal bound. Next, we will apply SQSLO in parallel and collective QB cases to further explore its behavior in those scenarios.

Having computed the QSLO for both parallel ($J = 0$) and collective charging ($J \neq 0$) QB cases, we will now apply the SQSLO bound in both these cases. This involves evaluation of $R(t)$ for both scenarios. We have already given the expression for collective charging ($J \neq 0$) case earlier. For parallel charging ($J = 0$) case with $\Omega = 1,\ \omega = 2$; this reads as

$$R(t) = \frac{1}{2}\left(2 + \frac{2\sqrt{10}\,\left|\sin(\sqrt{5}t)\right|\cot(\sqrt{5}t)}{\sqrt{9+\cos(2\sqrt{5}t)}}\right), \tag{64}$$

where the involved $|\Psi\rangle$ and $|\Psi^{\perp}\rangle$ in this case are given in Appendix B.

From the previous expressions, we reiterate that it appears that $|\Psi^{\perp}\rangle$ exhibits time dependence. However, according to the Heisenberg picture, the state should not evolve, indicating that we should not observe time dependence in the orthogonal state. Fundamentally, we acknowledge the existence of multiple choices for the orthogonal state of a given state. Therefore, we have adopted the most widely accepted method to select the orthogonal state to optimize our parameter R. In Eq. (38), we notice that the observable O is involved in the formula, and we employ its associated battery Hamiltonian $H_B(t)$, which evolves in the Heisenberg picture. Consequently, the time dependence on $|\Psi^{\perp}\rangle$ state arises. Through this selection, we achieve optimal value for the expression R.

Now, it is interesting to observe the behavior of SQSLO over a longer duration. We have plotted SQSLO for an extended period of time, and we observe optimal results, as illustrated in Fig. 9. Thus, one can affirm that for QB scenarios, SQSLO stands as the optimal choice—it represents the best bound for calculating the charging time of quantum batteries.

We have analyzed various quantum battery scenarios, including parallel, collective, coupling, and decoupling cases, and presented our findings for QSLO and SQSLO. It is evident that SQSLO consistently reveals the tightest bound for

quantum speed limit. Consequently, we can assert that SQSLO outperforms in predicting the charging time.

VI. CONCLUSION

In conclusion, we have addressed the fundamental question of how fast an observable can evolve in time by invoking the concept of the observable speed limit. Our study presents a stronger version of this limit, demonstrating that previously derived bounds are special cases of our new bound. We have also shown that SQSLO can lead to stronger speed limit for states. By applying SQSLO, we have investigated its efficacy in evaluating the capacity of entanglement, akin to the heat capacity in quantum information theory. Notably, we have established a more robust bound for the entanglement rate, surpassing previous limitations. Moreover, our exploration extends to the realm of interacting qubits within quantum batteries. By leveraging SQSLO, we have accurately predicted the time required to charge the battery, showcasing the tightness of SQSLO in this context—it effectively saturates when estimating the charging time of quantum batteries. These findings hold significant implications across various domains, including quantum thermodynamics, the complexity of operator growth, prediction of quantum correlation growth rates, and the broader landscape of quantum technology. Thus, SQSLO emerges as a powerful tool with diverse applications, paving the way for advancements in quantum science and technology.

ACKNOWLEDGMENTS

D.S. acknowledges the support of the INFOSYS scholarship. B.P. acknowledges IIIT, Hyderabad and TCG CREST (CQuERE) for their support and hospitality during the academic visit.

APPENDIX A: SQSL BOUND FOR ENTANGLEMENT CAPACITY

SQSL bound for entanglement generation using the capacity of entanglement under Schrödinger picture requires the functional form of $R(t)$ and $|\Psi^{\perp}\rangle$ as defined in Eq. (38)

$$R(t) = \frac{|\sqrt{-\text{arctanh}(\alpha)^2\beta}/\sqrt{2} + \text{arctanh}(\alpha)\ \text{Sign}[(1-2p)\theta]\ [-2i\sqrt{p(1-p)}\ \cos(2\theta t) - \sin(2\theta t)]|^2}{|\text{arctanh}(\alpha)^2\ \beta|}, \tag{A1}$$

where $\alpha = (2p-1)\cos(2\theta t)$, $\beta = -1 - 4p(1-p) + (1-2p)^2\cos(4\theta t)$. Also,

$$|\Psi^{\perp}\rangle = \begin{pmatrix} \frac{\sqrt{2}e^{-it\mu_3}\ \arctan\left[(-1+2p)\cos(2t\theta)\right](-1+(-1+2p)\cos(2t\theta))\left(\sqrt{p}\cos(t\theta)-i\sqrt{1-p}\sin(t\theta)\right)}{\sqrt{-\arctan\left[(-1+2p)\cos(2t\theta)\right]^2[-1+4(-1+p)p+(1-2p)^2\cos(4t\theta)]}} \\ 0 \\ 0 \\ \frac{\sqrt{2}e^{-it\mu_3}\ \arctan\left[(-1+2p)\cos(2t\theta)\right][1+(-1+2p)\cos(2t\theta)]\left(\sqrt{1-p}\cos(t\theta)-i\sqrt{p}\sin(t\theta)\right)}{\sqrt{-\arctan\left[(-1+2p)\cos(2t\theta)\right]^2[-1+4(-1+p)p+(1-2p)^2\cos(4t\theta)]}} \end{pmatrix}, \tag{A2}$$

where $\theta = (\mu_1 - \mu_2)$.

Similarly, SQSLO bound for generation of modular energy using the composite modular Hamiltonian under the Heisenberg picture requires the functional form of $R(t)$ and $|\Psi^{\perp}\rangle$ as defined in Eq. (38).

$$|\Psi^{\perp}\rangle = \begin{pmatrix} \frac{\log_2\left(-1+\frac{1}{p}\right)\left(-2(-1+p)\sqrt{p}\cos(2\theta t)-i\sqrt{1-p}\sin(2\theta t)\right)}{\sqrt{\log_2^2\left(-1+\frac{1}{p}\right)\left(-4(-1+p)p\cos^2(2\theta t)+\sin^2(2\theta t)\right)}} \\ 0 \\ 0 \\ \frac{\log_2\left(-1+\frac{1}{p}\right)\left(-2\sqrt{(1-p)p}\cos(2\theta t)+i\sin(2\theta t)\right)}{\sqrt{\frac{\log_2^2\left(-1+\frac{1}{p}\right)\left(-4(-1+p)p\cos^2(2\theta t)+\sin^2(2\theta t)\right)}{p}}} \end{pmatrix}, \tag{A3}$$

For $p = 0.1$ and $\Theta = 1$, R is given as:

$$R(t) = \frac{0.63|1.89 + \cos(2t)(1.67i\sqrt{0.68 - 0.32\cos(4t)}) - 0.89\cos(4t) + 2.78\sqrt{0.68 - 0.32\cos(4t)}\sin(2t)|^2}{[2.13 - \cos(4t)]^2}, \tag{A4}$$

Again, for $p = 0.1$ and $\Theta = 0.5$, R is given as:

$$R(t) = -\frac{0.15|\cos(t)^2 + \cos(t)(1.67i)\sqrt{0.68 - 0.32\cos(2t)}) + \sin(t)(2.78\sqrt{0.68 - 0.32\cos(2t)} + 2.78\sin(t))|^2}{-1.18 + \cos(2t) - 0.12\cos(4t)}, \tag{A5}$$

Again, for $p = 0.4$ and $\Theta = 1$, R is given as:

$$R(t) = 0.5\left|\frac{1}{(-49 + \cos(4t))}(-49 + \cos(4t) - (48.99i)\sqrt{0.98 - 0.02\cos(4t)}[\cos(2t) - (2.04i)\cos(t)\sin(t)])\right|^2, \tag{A6}$$

At last, for $p = 0.4$ and $\Theta = 0.5$, R is given as:

$$R(t) = -\frac{11.76|\cos(t)^2 + \cos(t)(-1.02i\sqrt{0.98 - 0.02\cos(2t)}) + \sin(t)(1.04\sqrt{0.98 - 0.02\cos(2t)} + 1.04\sin(t))|^2}{-24.51 + \cos(2t) - 0.005\cos(4t)}. \quad \text{(A7)}$$

APPENDIX B: RELATED TO QUANTUM BATTERY

There are three cases in which we have calculated the SQSLO for QBs. For each case, we require the values of $|\Psi\rangle$, and $|\Psi^{\perp}\rangle$. We will define each of these components individually.

Here, for all cases the initial state is

$$|\Psi\rangle = (0, 0, 0, 1)^T, \quad \text{(B1)}$$

For $J = 1$, $\omega = 2$ and $\Omega = 1$, the function $R(t)$ in Eq. (62), $|\Psi^{\perp}\rangle$ is provided below:

$$|\Psi^{\perp}\rangle = \begin{pmatrix} 0 \\ \frac{2-2\cos(2\sqrt{5}t)-i\sqrt{5}\sin(2\sqrt{5}t)}{2|\sin(\sqrt{5}t)|\sqrt{9+\cos(2\sqrt{5}t)}} \\ \frac{2-2\cos(2\sqrt{5}t)-i\sqrt{5}\sin(2\sqrt{5}t)}{2|\sin(\sqrt{5}t)|\sqrt{9+\cos(2\sqrt{5}t)}} \\ 0 \end{pmatrix}. \quad \text{(B2)}$$

For $J = 1$, $\omega = 2$ and $\Omega = 4$, the function $R(t)$ in Eq. (63), $\Psi^{\perp}\rangle$ is provided below:

$$|\Psi^{\perp}\rangle = \begin{pmatrix} 0 \\ \frac{1-\cos(4\sqrt{5}t)-t\sqrt{5}\sin(4\sqrt{5}t)}{2|\sin(2\sqrt{5}t)|\sqrt{6+4\cos(4\sqrt{5}t)}} \\ \frac{1-\cos(4\sqrt{5}t)-t=\sqrt{5}\sin(4\sqrt{5}t)}{2|\sin(2\sqrt{5}t)|\sqrt{6+4\cos(4\sqrt{5}t)}} \\ 0 \end{pmatrix}. \quad \text{(B3)}$$

For $J = 0$, $\omega = 2$ and $\Omega = 1$, the functions $R(t)$ in Eq. (64), $|\Psi^{\perp}\rangle$ is provided below:

$$|\Psi^{\perp}\rangle = \begin{pmatrix} 0 \\ \frac{e^{-2i+\sqrt{5}t}(-2+\sqrt{5}+4e^{2i+\sqrt{5}t}-(2+\sqrt{5})e^{4i\sqrt{5}t})}{4|\sin(\sqrt{5}\ t)|\sqrt{9+\cos(2\sqrt{5}t)}} \\ \frac{e^{-2i+\sqrt{5}t}(-2+\sqrt{5}+4e^{2i+\sqrt{5}t}-(2+\sqrt{5})e^{4+\sqrt{5}t})}{4|\sin(\sqrt{5}\ t)|\sqrt{9+\cos(2\sqrt{5}t)}} \\ 0 \end{pmatrix}. \quad \text{(B4)}$$

[1] L. Mandelstam and I. G. Tamm, The uncertainty relation between energy and time in non-relativistic quantum mechanics, J. Phys. (USSR) **9**, 249 (1945).

[2] A. K. Pati, Relation between phases and distance in quantum evolution, Phys. Lett. A **159**, 105 (1991).

[3] N. Margolus and L. B. Levitin, The maximum speed of dynamical evolution, Physica D **120**, 188 (1998).

[4] S. Bao, S. Kleer, R. Wang, and A. Rahmani, Optimal control of superconducting gmon qubits using Pontryagin's minimum principle: Preparing a maximally entangled state with singular bang-bang protocols, Phys. Rev. A **97**, 062343 (2018).

[5] R. R. Rodríguez, B. Ahmadi, G. Suárez, P. Mazurek, S. Barzanjeh, and P. Horodecki, Optimal quantum control of charging quantum batteries, New J. Phys. **26**, 043004 (2024).

[6] V. Evangelakos, E. Paspalakis, and D. Stefanatos, Minimum-time generation of a uniform superposition in a qubit with only transverse field control, Phys. Rev. A **108**, 062425 (2023).

[7] F. Mazzoncini, V. Cavina, G. M. Andolina, P. A. Erdman, and V. Giovannetti, Optimal control methods for quantum batteries, Phys. Rev. A **107**, 032218 (2023).

[8] J. Anandan and Y. Aharonov, Geometry of quantum evolution, Phys. Rev. Lett. **65**, 1697 (1990).

[9] L. B. Levitin and T. Toffoli, Fundamental limit on the rate of quantum dynamics: The unified bound is tight, Phys. Rev. Lett. **103**, 160502 (2009).

[10] E. A. Gislason, N. H. Sabelli, and J. W. Wood, New form of the time-energy uncertainty relation, Phys. Rev. A **31**, 2078 (1985).

[11] J. H. Eberly and L. P. S. Singh, Time operators, partial stationarity, and the energy-time uncertainty relation, Phys. Rev. D **7**, 359 (1973).

[12] M. Bauer and P. A. Mello, The time-energy uncertainty relation, Ann. Phys. (NY) **111**, 38 (1978).

[13] K. Bhattacharyya, Quantum decay and the Mandelstam-Tamm-energy inequality, J. Phys. A: Math. Gen. **16**, 2993 (1983).

[14] C. Leubner and C. Kiener, Improvement of the Eberly-Singh time-energy inequality by combination with the mandelstam-tamm approach, Phys. Rev. A **31**, 483 (1985).

[15] L. Vaidman, Minimum time for the evolution to an orthogonal quantum state, Am. J. Phys. **60**, 182 (1992).

[16] A. Uhlmann, An energy dispersion estimate, Phys. Lett. A **161**, 329 (1992).

[17] J. B. Uffink, The rate of evolution of a quantum state, Am. J. Phys. **61**, 935 (1993).

[18] P. Pfeifer and J. Fröhlich, Generalized time-energy uncertainty relations and bounds on lifetimes of resonances, Rev. Mod. Phys. **67**, 759 (1995).

[19] N. Horesh and A. Mann, Intelligent states for the Anandan - Aharonov parameter-based uncertainty relation, J. Phys. A: Math. Gen. **31**, L609 (1998).

[20] A. K. Pati, Uncertainty relation of Anandan-Aharonov and intelligent states, Phys. Lett. A **262**, 296-301 (1999).

[21] J. Söderholm, G. Björk, T. Tsegaye, and A. Trifonov, States that minimize the evolution time to become an orthogonal state, Phys. Rev. A **59**, 1788 (1999).

[22] M. Andrecut and M. K. Ali, The adiabatic analogue of the Margolus-Levitin theorem, J. Phys. A: Math. Gen. **37**, L157 (2004).

[23] J. E. Gray and A. Vogt, Mathematical analysis of the Mandelstam-Tamm time-energy uncertainty principle, J. Math. Phys. **46**, 052108 (2005).

[24] B. Zieliński and M. Zych, Generalization of the Margolus-Levitin bound, Phys. Rev. A **74**, 034301 (2006).

[25] M. Andrews, Bounds to unitary evolution, Phys. Rev. A **75**, 062112 (2007).

[26] U. Yurtsever, Fundamental limits on the speed of evolution of quantum states, Phys. Scr. **82**, 035008 (2010).
[27] F. Shuang-Shuang, L. Nan, and L. Shun-Long, A note on fundamental limit of quantum dynamics rate, Commun. Theor. Phys. **54**, 661 (2010).
[28] P. M. Poggi, F. C. Lombardo, and D. A. Wisniacki, Quantum speed limit and optimal evolution time in a two-level system, Europhys. Lett. **104**, 40005 (2013).
[29] J. Kupferman and B. Reznik, Entanglement and the speed of evolution in mixed states, Phys. Rev. A **78**, 042305 (2008).
[30] P. J. Jones and P. Kok, Geometric derivation of the quantum speed limit, Phys. Rev. A **82**, 022107 (2010).
[31] H. F. Chau, Tight upper bound of the maximum speed of evolution of a quantum state, Phys. Rev. A **81**, 062133 (2010).
[32] S. Deffner and E. Lutz, Energy-time uncertainty relation for driven quantum systems, J. Phys. A: Math. Theor. **46**, 335302 (2013).
[33] C.-H. F. Fung and H. F. Chau, Relation between physical time-energy cost of a quantum process and its information fidelity, Phys. Rev. A **90**, 022333 (2014).
[34] O. Andersson and H. Heydari, Quantum speed limits and optimal Hamiltonians for driven systems in mixed states, J. Phys. A: Math. Theor. **47**, 215301 (2014).
[35] D. Mondal, C. Datta, and S. Sazim, Quantum coherence sets the quantum speed limit for mixed states, Phys. Lett. A **380**, 689 (2016).
[36] D. Mondal and A. K. Pati, Quantum speed limit for mixed states using an experimentally realizable metric, Phys. Lett. A **380**, 1395 (2016).
[37] S. Deffner and S. Campbell, Quantum speed limits: from Heisenberg's uncertainty principle to optimal quantum control, J. Phys. A: Math. Theor. **50**, 453001 (2017).
[38] F. Campaioli, F. A. Pollock, F. C. Binder, and K. Modi, Tightening quantum speed limits for almost all states, Phys. Rev. Lett. **120**, 060409 (2018).
[39] S. Ashhab, P. C. de Groot, and F. Nori, Speed limits for quantum gates in multiqubit systems, Phys. Rev. A **85**, 052327 (2012).
[40] C. Mukhopadhyay, A. Misra, S. Bhattacharya, and A. K. Pati, Quantum speed limit constraints on a nanoscale autonomous refrigerator, Phys. Rev. E **97**, 062116 (2018).
[41] K. Funo, N. Shiraishi, and K. Saito, Speed limit for open quantum systems, New J. Phys. **21**, 013006 (2019).
[42] T. Caneva, M. Murphy, T. Calarco, R. Fazio, S. Montangero, V. Giovannetti, and G. E. Santoro, Optimal control at the quantum speed limit, Phys. Rev. Lett. **103**, 240501 (2009).
[43] S. Campbell and S. Deffner, Trade-off between speed and cost in shortcuts to adiabaticity, Phys. Rev. Lett. **118**, 100601 (2017).
[44] S. Campbell, M. G. Genoni, and S. Deffner, Precision thermometry and the quantum speed limit, Quantum Sci. Technol. **3**, 025002 (2018).
[45] L. Maccone and A. K. Pati, Stronger uncertainty relations for all incompatible observables, Phys. Rev. Lett. **113**, 260401 (2014).
[46] D. Thakuria and A. K. Pati, Stronger quantum speed limit, arXiv:2208.05469.
[47] B. Mohan and A. K. Pati, Quantum speed limits for observables, Phys. Rev. A **106**, 042436 (2022).
[48] R. Horodecki, P. Horodecki, M. Horodecki, and K. Horodecki, Quantum entanglement, Rev. Mod. Phys. **81**, 865 (2009).
[49] S. Das, T. Chanda, M. Lewenstein, A. Sanpera, A. Sen De, and U. Sen, The separability versus entanglement problem, Quant. Inf., 127 (2016).
[50] J. de Boer, J. Järvelä, and E. Keski-Vakkuri, Aspects of capacity of entanglement, Phys. Rev. D **99**, 066012 (2019).
[51] D. Shrimali, S. Bhowmick, V. Pandey, and A. K. Pati, Capacity of entanglement for a nonlocal Hamiltonian, Phys. Rev. A **106**, 042419 (2022).
[52] N. Laflorencie, Quantum entanglement in condensed matter systems, Phys. Rep. **646**, 1 (2016).
[53] H. Yao and X.-L. Qi, Entanglement entropy and entanglement spectrum of the Kitaev model, Phys. Rev. Lett. **105**, 080501 (2010).
[54] R. Alicki and M. Fannes, Entanglement boost for extractable work from ensembles of quantum batteries, Phys. Rev. E **87**, 042123 (2013).
[55] F. C. Binder, S. Vinjanampathy, K. Modi, and J. Goold, Quantacell: Powerful charging of quantum batteries, New J. Phys. **17**, 075015 (2015).
[56] F. Campaioli, F. A. Pollock, F. C. Binder, L. Céleri, J. Goold, S. Vinjanampathy, and K. Modi, Enhancing the charging power of quantum batteries, Phys. Rev. Lett. **118**, 150601 (2017).
[57] D. Rossini, G. M. Andolina, D. Rosa, M. Carrega, and M. Polini, Quantum advantage in the charging process of Sachdev-Ye-Kitaev batteries, Phys. Rev. Lett. **125**, 236402 (2020).
[58] J.-Y. Gyhm, D. Šafránek, and D. Rosa, Quantum charging advantage cannot be extensive without global operations, Phys. Rev. Lett. **128**, 140501 (2022).
[59] J.-Y. Gyhm and U. R. Fischer, Beneficial and detrimental entanglement for quantum battery charging, AVS Quantum Science **6**, 012001 (2024).
[60] J.-Y. Gyhm, D. Rosa, and D. Šafránek, Minimal time required to charge a quantum system, Phys. Rev. A **109**, 022607 (2024).
[61] S. Julià-Farré, T. Salamon, A. Riera, M. N. Bera, and M. Lewenstein, Bounds on the capacity and power of quantum batteries, Phys. Rev. Res. **2**, 023113 (2020).
[62] F. Campaioli, S. Gherardini, J. Q. Quach, M. Polini, and G. M. Andolina, *Colloquium*: Quantum batteries, Rev. Mod. Phys. **96**, 031001 (2024).
[63] G. M. Andolina, D. Farina, A. Mari, V. Pellegrini, V. Giovannetti, and M. Polini, Charger-mediated energy transfer in exactly solvable models for quantum batteries, Phys. Rev. B **98**, 205423 (2018).
[64] T. P. Le, J. Levinsen, K. Modi, M. M. Parish, and F. A. Pollock, Spin-chain model of a many-body quantum battery, Phys. Rev. A **97**, 022106 (2018).
[65] Y.-Y. Zhang, T.-R. Yang, L. Fu, and X. Wang, Powerful harmonic charging in a quantum battery, Phys. Rev. E **99**, 052106 (2019).
[66] F. Barra, Dissipative charging of a quantum battery, Phys. Rev. Lett. **122**, 210601 (2019).
[67] A. C. Santos, B. Çakmak, S. Campbell, and N. T. Zinner, Stable adiabatic quantum batteries, Phys. Rev. E **100**, 032107 (2019).
[68] G. M. Andolina, M. Keck, A. Mari, M. Campisi, V. Giovannetti, and M. Polini, Extractable work, the role of cor-

relations, and asymptotic freedom in quantum batteries, Phys. Rev. Lett. **122**, 047702 (2019).
[69] A. Crescente, M. Carrega, M. Sassetti, and D. Ferraro, Ultrafast charging in a two-photon Dicke quantum battery, Phys. Rev. B **102**, 245407 (2020).
[70] A. C. Santos, A. Saguia, and M. S. Sarandy, Stable and charge-switchable quantum batteries, Phys. Rev. E **101**, 062114 (2020).
[71] A. C. Santos, Quantum advantage of two-level batteries in the self-discharging process, Phys. Rev. E **103**, 042118 (2021).
[72] F.-Q. Dou, Y.-Q. Lu, Y.-J. Wang, and J.-A. Sun, Extended dicke quantum battery with interatomic interactions and driving field, Phys. Rev. B **105**, 115405 (2022).
[73] F. Barra, K. V. Hovhannisyan, and A. Imparato, Quantum batteries at the verge of a phase transition, New J. Phys. **24**, 015003 (2022).
[74] J. Carrasco, J. R. Maze, C. Hermann-Avigliano, and F. Barra, Collective enhancement in dissipative quantum batteries, Phys. Rev. E **105**, 064119 (2022).
[75] V. Shaghaghi, V. Singh, G. Benenti, and D. Rosa, Micromasers as quantum batteries, Quantum Sci. Technol. **7**, 04LT01 (2022).
[76] C. Rodríguez, D. Rosa, and J. Olle, Artificial intelligence discovery of a charging protocol in a micromaser quantum battery, Phys. Rev. A **108**, 042618 (2023).
[77] T. F. F. Santos, Y. V. de Almeida, and M. F. Santos, Vacuum-enhanced charging of a quantum battery, Phys. Rev. A **107**, 032203 (2023).
[78] F. H. Kamin, Z. Abuali, H. Ness, and S. Salimi, Quantum battery charging by non-equilibrium steady-state currents, J. Phys. A: Math. Theor. **56**, 275302 (2023).
[79] C. A. Downing and M. S. Ukhtary, A quantum battery with quadratic driving, Commun. Phys. **6**, 322 (2023).
[80] M. Hadipour, S. Haseli, D. Wang, and S. Haddadi, Practical scheme for realization of a quantum battery, arXiv:2312.06389.
[81] F. T. Tabesh, F. H. Kamin, and S. Salimi, Environment-mediated charging process of quantum batteries, Phys. Rev. A **102**, 052223 (2020).
[82] F. H. Kamin, F. T. Tabesh, S. Salimi, and A. C. Santos, Entanglement, coherence, and charging process of quantum batteries, Phys. Rev. E **102**, 052109 (2020).
[83] F. Pirmoradian and K. Mølmer, Aging of a quantum battery, Phys. Rev. A **100**, 043833 (2019).
[84] X. Zhang and M. Blaauboer, Enhanced energy transfer in a Dicke quantum battery, Front. Phys. **10** (2023).
[85] A. Crescente, M. Carrega, M. Sassetti, and D. Ferraro, Charging and energy fluctuations of a driven quantum battery, New J. Phys. **22**, 063057 (2020).
[86] J. Joshi and T. S. Mahesh, Experimental investigation of a quantum battery using star-topology NMR spin systems, Phys. Rev. A **106**, 042601 (2022).
[87] B. Mohan and A. K. Pati, Reverse quantum speed limit: How slowly a quantum battery can discharge, Phys. Rev. A **104**, 042209 (2021).
[88] W. Niedenzu, V. Mukherjee, A. Ghosh, A. G. Kofman, and G. Kurizki, Quantum engine efficiency bound beyond the second law of thermodynamics, Nat. Commun. **9**, 165 (2018).
[89] D. Ferraro, M. Campisi, G. M. Andolina, V. Pellegrini, and M. Polini, High-power collective charging of a solid-state quantum battery, Phys. Rev. Lett. **120**, 117702 (2018).
[90] F. Zhao, F.-Q. Dou, and Q. Zhao, Quantum battery of interacting spins with environmental noise, Phys. Rev. A **103**, 033715 (2021).
[91] D. Rossini, G. M. Andolina, and M. Polini, Many-body localized quantum batteries, Phys. Rev. B **100**, 115142 (2019).
[92] S. Zakavati, F. T. Tabesh, and S. Salimi, Bounds on charging power of open quantum batteries, Phys. Rev. E **104**, 054117 (2021).
[93] F. Zhao, F.-Q. Dou, and Q. Zhao, Charging performance of the Su-Schrieffer-Heeger quantum battery, Phys. Rev. Res. **4**, 013172 (2022).
[94] J. Q. Quach, K. E. McGhee, L. Ganzer, D. M. Rouse, B. W. Lovett, E. M. Gauger, J. Keeling, G. Cerullo, D. G. Lidzey, and T. Virgili, Superabsorption in an organic microcavity: Toward a quantum battery, Sci. Adv. **8**, eabk3160 (2022).
[95] N. Carabba, N. Hörnedal, and A. D. Campo, Quantum speed limits on operator flows and correlation functions, Quantum **6**, 884 (2022).
[96] P. Caputa, J. M. Magan, and D. Patramanis, Geometry of Krylov complexity, Phys. Rev. Res. **4**, 013041 (2022).
[97] V. Pandey, D. Shrimali, B. Mohan, S. Das, and A. K. Pati, Speed limits on correlations in bipartite quantum systems, Phys. Rev. A **107**, 052419 (2023).
[98] A. K. Pati, B. Mohan, Sahil, and S. L. Braunstein, Exact quantum speed limits, arXiv:2305.03839.
[99] W. Dür, G. Vidal, J. I. Cirac, N. Linden, and S. Popescu, Entanglement capabilities of nonlocal Hamiltonians, Phys. Rev. Lett. **87**, 137901 (2001).
[100] C. H. Bennett, J. I. Cirac, M. S. Leifer, D. W. Leung, N. Linden, S. Popescu, and G. Vidal, Optimal simulation of two-qubit Hamiltonians using general local operations, Phys. Rev. A **66**, 012305 (2002).
[101] A. K. Pati, New derivation of the geometric phase, Phys. Lett. A **202**, 40 (1995).
[102] S. Bravyi, Upper bounds on entangling rates of bipartite Hamiltonians, Phys. Rev. A **76**, 052319 (2007).
[103] P. Pfeifer, How fast can a quantum state change with time? Phys. Rev. Lett. **70**, 3365 (1993).
[104] S.-x. Wu and C.-s. Yu, Quantum speed limit for a mixed initial state, Phys. Rev. A **98**, 042132 (2018).
[105] F. Campaioli, C. shui Yu, F. A. Pollock, and K. Modi, Resource speed limits: Maximal rate of resource variation, New J. Phys. **24**, 065001 (2022).
[106] D. Thakuria, A. Srivastav, B. Mohan, A. Kumari, and A. K. Pati, Generalised quantum speed limit for arbitrary time-continuous evolution, J. Phys. A: Math. Theor. **57**, 025302 (2024).
[107] B. Mohan, S. Das, and A. K. Pati, Quantum speed limits for information and coherence, New J. Phys. **24**, 065003 (2022).
[108] R Alicki, The quantum open system as a model of the heat engine, J. Phys. A: Math. Gen. **12**, L103 (1979).
[109] F. Campaioli, F. A. Pollock, and S. Vinjanampathy, Quantum batteries, in *Thermodynamics in the Quantum Regime: Fundamental Aspects and New Directions*, edited by F. Binder, L. A. Correa, C. Gogolin, J. Anders, and G. Adesso (Springer, Cham, 2019), Vol. 195, pp. 207–225.